- 1 A biological effect-guided optimization approach using beam
- 2 distal-edge avoidance for intensity-modulated proton therapy

4 Xuemin Bai<sup>1,2</sup>, Gino Lim<sup>1</sup>, David Grosshans<sup>3</sup>, Radhe Mohan<sup>4</sup>, Wenhua Cao<sup>4</sup>

5

- <sup>1</sup>Department of Industrial Engineering, University of Houston, Houston, TX, United
- 7 States of America
- 8 <sup>2</sup>Linking Medical Technology, Beijing, China
- <sup>3</sup>Department of Radiation Oncology, The University of Texas MD Anderson Cancer
- 10 Center, Houston, TX, United States of America
- <sup>4</sup>Department of Radiation Physics, The University of Texas MD Anderson Cancer Center,
- 12 Houston, TX, United States of America
- 13 **Running title:** Biological effect optimization in IMPT
- 14 Corresponding author: Wenhua Cao, wcao1@mdanderson.org

### **ABSTRACT**

16

**Purpose**: Linear energy transfer (LET)-guided methods have been applied to 17 intensity-modulated proton therapy (IMPT) to improve its biological effect. However, 18 using LET as a surrogate for biological effect ignores the topological relationship of the 19 scanning spot to different structures of interest. In this study, we developed an 20 optimization method that takes advantage of the continuing increase in LET beyond the 21 physical dose Bragg peak. This method avoids placing high biological-effect values in 22 critical structures and increases biological effect in the tumor area without compromising 23 target coverage. 24 **Methods**: We selected the cases of two patients with brain tumors and two patients with 25 head and neck tumors who had been treated with proton therapy at our institution. Three 26 27 plans were created for each case: a plan based on conventional dose-based optimization (DoseOpt), one based on LET-incorporating optimization (LETOpt), and one based on 28 29 the proposed distal-edge avoidance-guided optimization method (DEAOpt). In DEAOpt, an  $L_l$ -norm sparsity term, in which the penalty of each scanning spot was set according to 30 the topological relationship between the organ positions and the location of the peak 31 scaled LET-weighted dose (c LETxD) was added to a conventional dose-based 32 33 optimization objective function. All plans were normalized to give the same target dose coverage. Dose (assuming a constant relative biological effectiveness value of 1.1, as in 34 clinical practice), biological effect (c LETxD), and computing time consumption were 35 evaluated and compared among the three optimization approaches for each patient case. 36

37 **Results**: For all four cases, all three optimization methods generated comparable dose

coverage in both target and critical structures. The LETOpt plans and DEAOpt plans

reduced biological-effect hot spots in critical structures and increased biological effect in

40 the target volumes to a similar extent. For the target, the c LETxD<sub>98%</sub> and c LETxD<sub>2%</sub> in

the DEAOpt plans were on average 7.2% and 11.74% higher than in the the DoseOpt

plans, respectively. For the brainstem, the c LETxD<sub>mean</sub> in the DEAOpt plans was on

average 33.38% lower than in the DoseOpt plans. In addtion, the DEAOpt method saved

44 30.37% of the computation cost over the LETOpt method.

45 **Conclusions**: DEAOpt is an alternative IMPT optimization approach that correlates the

location of scanning spots with biological effect distribution. IMPT could benefit from

the use of DEAOpt because this method not only delivers comparable biological effects

48 to LETOpt plans, but also is faster.

49

47

39

41

43

50 **Key words:** IMPT, biological effect, LET, RBE

### 1. INTRODUCTION

52

Proton beams deposit dose slowly along their incoming path before reaching a sharp peak 53 known as the Bragg peak. Beyond the Bragg peak, the deposited dose rapidly falls to 54 almost zero. This physical property of proton beams enables intensity-modulated proton 55 therapy (IMPT): delivery of a highly conformal dose enclosing the tumor while sparing 56 adjacent normal tissue. In addition, the biological effect of proton beams is greater than 57 that of photons. Biological effect is usually measured by the relative biological 58 effectiveness (RBE), i.e., the ratio of the doses of two types of ionizing radiation needed 59 to reach the same biological effect.<sup>2,3</sup> A constant RBE value of 1.1 (i.e., 10% more 60 effective than a photon beam) is currently used in recommendations for clinical proton 61 treatment planning from the International Commission on Radiation Units and 62 Measurements.4 63 64 65 RBE varies depending on linear energy transfer (LET), tissue-specific parameters (defined by  $\alpha$  and  $\beta$ ), dose per fraction, and other factors. <sup>2,5–8</sup> However, existing 66 experimental biological data are insufficient to clearly correlate RBE and dose per 67 fraction or  $(\alpha/\beta)_x$  for *in vivo* endpoints.<sup>2,9,10</sup> Therefore, use of these variable RBE models 68 to evaluate proton treatment plans may lead to unwanted clinical consequences. For 69 example, if the calculation of the target dose coverage is based on a variable 70 RBE-weighted dose, the patient will be at risk of receiving a lower physical dose in parts 71 of the tumor because variable RBE is assumed to be greater than 1.1 in areas of high LET. 72

Critical structures are in danger of being exposed to a higher physical dose when the

variable RBE is underestimated. 11,12

75

To resolve this problem, recent studies have attempted to optimize a biological dose 76 approximated by both physcial dose and LET. This is because the biological effectiveness 77 78 of a proton beam increases with the increase in LET toward the end of the proton range. 11,13 LET can be predicted precisely using analytical methods or Monte Carlo 79 simulations. 14 Several studies have developed methods to take advantage of LET to 80 maximize biological effectiveness in proton therapy. In order to increase LET to achieve 81 a higher biological effect in radioresistant tumors, Bassler et al. 15 introduced a 82 "LET-painting" method that can generate mixed-modality treatment plans using protons 83 and carbon ions to shape a high-LET region throughout the planning target volume. Fager 84 et al. 13 used multiple radiation fields to cover different segments of the target so that the 85 dose prescriptions could be reduced by the increased LET in the target. Tseung et al. 16 86 took advantage of graphics processing unit acceleration to optimize the biological dose 87 for head and neck cancer cases. To reduce the risk of normal tissue complications, 88 Unkelbach et al. 11 applied a two-step optimization method to avoid high scaled 89 LET-weighted dose values in critical structures. To reduce LET and RBE in organs at risk 90 (OARs), Traneus and Ödén<sup>17</sup> noticed the location of the proton track-end and added it 91 into an objective function. 92

Various LET optimization techniques have also been developed to optimize the biological effect in both target volumes and critical structures. Giantsoudi et al. 18 presented a multicriteria optimization method to find plans with higher dose-averaged LET (LET<sub>d</sub>) in tumor targets and lower LET<sub>d</sub> in normal tissue structures. Inaniwa et al. 19 minimized the physical dose and LET<sub>d</sub> based on prescribed values in a quadratic cost function, while Cao et al.<sup>20</sup> added two terms for maximizing LET-weighted dose in the target and minimizing it in OARs without considering any prescription. To deal with plan robustness under proton range and patient setup uncertainties. An et al.<sup>21</sup> minimized the highest LET in OARs while maintaining the same dose coverage and robustness in tumor targets as the conventional robust IMPT treatment plan model, while Bai et al.<sup>22</sup> penalized the sum of the differences between the highest and lowest biological effect in each voxel, approximated by the product of dose and LET, to achieve robust biological effect and physical dose distributions in both target and critical structures. However, these approaches typically used optimization priorities to control the trade-off dynamic between dose and LET criteria. The interrelationship between dose and LET of protons was not incorporated in the objectives or constraints.

110

111

112

113

114

94

95

96

97

98

99

100

101

102

103

104

105

106

107

108

109

Notably, LET keeps increasing beyond the location of the Bragg peak in the patient volume. This property could be explicitly considered in optimization. Therefore, we investigated the impact of directly including the scanning spot position in IMPT optimization. We introduced an influence index for each scanning spot based on its

topological relationship to different organs of interest and added this index to a conventional dose-based objective function. Both physical dose and LET distributions can be optimized simultaneously in the proposed approach.

118

119

115

116

117

### 2. MATERIALS AND METHODS

- 120 This work evaluated the effectiveness of distal-edge avoidance-guided optimization
- 121 (DEAOpt) by comparing its results with those of conventional dose-based optimization
- 122 (DoseOpt) and LET-incorporating optimization (LETOpt) using four clinical cases.

123

## 2.A. Distal-edge avoidance-guided optimization (DEAOpt)

- 125 IMPT treatment planning using the 3D spot scanning technique<sup>23</sup> can deposit physical
- dose  $D_{ij}$  and LET  $L_{ij}$  to voxel i by the  $j^{th}$  beamlet with unit intensity. The total dose
- 127  $(D_i)$ , LET<sub>d</sub>  $(L_i)$ , and LET-weighted dose or LETxD  $(LD_i)$  in the voxel i are calculated
- 128 by:

$$D_{i} = \sum_{j}^{N_{B}} D_{ij} w_{j}^{2} \tag{1}$$

130 
$$L_{i} = \frac{\sum_{j}^{N_{B}} D_{ij} L_{ij} w_{j}^{2}}{\sum_{j}^{N_{B}} D_{ij} w_{j}^{2}}$$
 (2)

131 and

$$LD_i = \sum_{j}^{N_B} D_{ij} L_{ij} w_j^2 \tag{3}$$

- respectively, where  $w_j^2$  is the intensity of beamlet j among beamlet set  $N_B$  to preserve
- the nonnegativity. The dose and LET calculations in this study were performed with

matRad, an open-source treatment planning platform.<sup>24</sup> Dose was calculated based on a pencil beam algorithm using tabulated depth dose curves for individual particle energies and Gaussian sigma for lateral broadening.<sup>25</sup> Each voxel's LET was also calculated based on an analytical algorithm for depth direction and with constant LET laterally.<sup>14</sup>

139

140

141

142

143

144

135

136

137

138

- For DoseOpt, a standard quadratic objective function was used to minimize the mean square deviation between the calculated dose distribution and the ideal prescription over the entire volume.<sup>26</sup> Different weighting factors,  $\lambda_T$  and  $\lambda_{OAR}$ , and prescription values,  $D_{0,T}$  and  $D_{0,OAR}$ , for the structures were applied to control the balance between target coverage and critical structure sparing. The objective function is given by<sup>27</sup>:
- 145  $F_N(w_j) = \lambda_T \frac{1}{N_T} \sum_{i=1}^{N_T} (D_i D_{0,T})^2 + \lambda_{OAR} \frac{1}{N_{OAR}} \sum_{i=1}^{N_{OAR}} H(D_i D_{0,OAR}) \times (D_i D_{0,OAR})^2$
- 146 (4)
- Here,  $N_T$  and  $N_{OAR}$  are the sets of voxels in target volumes and OARs, respectively.
- The Heaviside function, denoted by  $H(D_i D_{0,OAR})$ , is a discontinuous function whose
- value is zero if  $D_i \le D_{0,OAR}$  and one if  $D_i > D_{0,OAR}$ .

- Because the scaled LETxD (c LETxD) can be regarded as the additional biological dose contributed by the LET effect,<sup>11</sup> two LETxD terms were added to Function (4) to maximize the biological dose in the target and minimize it in the OARs for the LETOpt.<sup>11,19,20</sup> The optimization weighting factors for the two objective terms were  $\theta_T$
- and  $\theta_{OAR}$ . The cost function of LETOpt was formulated as shown in (5):

156  $F_L(w_j) = F_N(w_j) - \theta_T \frac{1}{N_T} \sum_{i=1}^{N_T} cLD_i^2 + \theta_{OAR} \frac{1}{N_{OAR}} \sum_{i=1}^{N_{OAR}} cLD_i^2$  (5)

The scaling factor c was set to 0.04  $\mu m/KeV$  in this study. According to Unkelbach et al., 11 a threshold value  $LD^{ref}$ , such that 95% of the target volume receives  $LD_i$  values higher than LD<sup>ref</sup>, can be used for normal tissues. In our case, we did not involve the prescriptions for the LETxD terms  $(LD^{ref})$  because there was a large difference in the LET distributions for different cases, and even for the same case with different beam angles. Our goal was to increase the biological dose in the target and reduce it in OARs as much as possible. Because increasing the biological dose in the target often comes at the cost of increasing the biological dose in the OARs, one can adjust the weighting factors ( $\theta_T$  and  $\theta_{OAR}$ ) in Formulation (5) to find a balance between the target and the OARs. However, the threshold  $LD^{ref}$  can easily be added to Formulation (5) for both the target and critical structures. It should also be noted that setting the weighting factors for LETxD in LETOpt is based on trial and error, the same process whereas setting ones for dose in standard optimization (DoseOpt). The both types of factors ( $\lambda$  and  $\theta$ ) should be within the same scale. In practice, if standard optimization were performed first with preferred setting of  $\lambda$ , one only needs to adjust  $\theta$  and keep the same  $\lambda$  for LET optimization.

173

174

175

176

157

158

159

160

161

162

163

164

165

166

167

168

169

170

171

172

The proton beam energy was chosen so that the Bragg peak of the depth dose curve coincided with the distal target edge. Since LET keeps rising beyond the Bragg peak, the highest value of the LETxD appeared at position  $p_i$ , which is a distance  $d_i$  away

from the scanning spot location  $s_j$  along the beam direction  $\overrightarrow{b_j}$ . This distance depends on the beam energy and tissue type.

$$p_j = s_j + \overrightarrow{b_j} \cdot d_j \tag{6}$$

In order to limit high biological dose in the target area and protect critical structures, we examined the topological relationship between the peak LETxD position, the target location, and the critical structure locations in four situations, shown in Figure 1. For Situation A, the position of the peak LETxD value  $p_j$  falls into the OAR areas and outside the target region; a penalty  $\theta_A$  was assigned to this beamlet. For Situation B, where  $p_j$  is in the overlap area of the target and OAR,  $\theta_B$  was the assigned penalty. For Situation C, where a subregion formed by the center  $p_j$  and semidiameter  $R_j$  overlaps with an OAR but not the target area, the penalty was  $\theta_C$ . Finally, in Situation D, where the subregion is outside the OAR and overlaps with the target volume, the penalty was  $\theta_D$ .

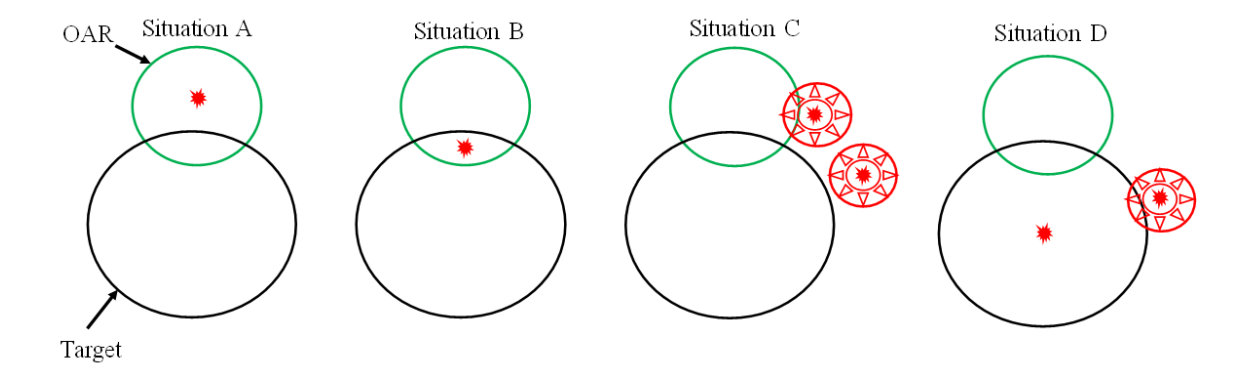


Figure 1. Topological relationship between peak locations of scaled linear energy transfer-weighted dose and different structures.

194 The semidiameter  $R_j$  is the proximal 80% to distal width of the most distal peak of 195 beamlet j.<sup>28,29</sup> The values of penalty  $\theta$  were set based on Formulation (7) and case 196 preferences, i.e.,  $\theta_j \in \{\theta_A, \theta_C, \theta_B, \theta_D\}$ . Note that the location of peak LETxD was 197 determined according to calculated LETxD from  $D_i$  and  $L_i$  before optimization.

$$\theta_A \ge \theta_C \ge \theta_B \ge \theta_D \tag{7}$$

199

204

205

206

207

208

Thus, we added an  $L_1$ -norm sparsity term, in which the penalty for beamlet intensity was based on the topological relationship shown above, to Formulation (4) to construct the objective function for the DEAOpt:

203 
$$F_S(w_j) = F_N(w_j) + \frac{1}{N_B} \sum_{j=1}^{N_B} \theta_j w_j^2$$
 (8)

The setting of  $\theta_j$  for those spots flagged by the 4 situations described above is based on trial and error in order to adjust the tradeoff effect between this spot penalty with dose criteria, besides the order of possible values set by (7). For example, if the treating physician preferred to maintain a high biological dose in the area where the target and OARs overlap, a low value of  $\theta_B$  was assigned.

209

210

211

In this study, the DoseOpt, LETOpt, and DEAOpt models were solved by IPOPT,<sup>30</sup> an optimizer based on interior-point methods for nonlinear optimization problems.

212

## 2.B. Patient data and treatment planning

Table 1. Patient information and treatment planning parameters

Tumor location	Prescription dose (Gy/fx)	Number of fractions	Beam angles (gantry, couch)	Number of beamlets	Volumes included in optimization
1. Brain	1.8 (CTV)	30	(260, 0)	1813	CTV, PTV, brainstem,
			(100, 0)	1829	optic chiasm, spinal cord, brain
			(180, 0)	1826	
2. Brain	1.8 (CTV)	30	(265, 90)	1417	CTV, PTV, brainstem,
			(260, 0)	1388	optic chiasm, spinal cord, brain
			(100, 0)	1410	
			(180, 0)	1335	
3. H&N	2.0 (CTV)	33	(180, 0)	2505	CTV, parotid, larynx, spinal cord,
			(65, 345)	2800	mandible, cochlea, brainstem,
			(300, 20)	2580	esophagus
4. H&N	2.0 (CTV)	33	(300, 15)	4123	CTV, parotid, larynx, spinal cord,
			(60, 345)	4217	mandible, cochlea, brainstem,
			(180, 0)	4114	esophagus

Abbreviations: CTV, clinical target volume; PTV, planning target volume; H&N, head and neck

We implemented the proposed DEAOpt method, the conventional DoseOpt method, and the LETOpt method in four clinical cases retrospectively selected from our patient database: two patients with brain cancer and two with head-and-neck (H&N) cancer. For brain tumor patients, a prescribed dose of 1.8 Gy (RBE = 1.1) per fraction to the target volumes was planned in 30 fractions. The prescription dose of 2.0 Gy (RBE = 1.1) per fraction to the target volumes was applied for H&N cancer patients in 33 fractions. To simplify the problem, the doses prescribed to OARs were set to 0 in the optimizations. For all patients, beam angles were the same as those used in the clinical treatment. Although the target volume and location varied among the patient cases, at least one critical structure was close to or overlapped with the clinical target volumes (CTVs) or

the planning target volumes (PTVs) in each case. More planning details are listed in Table 1.

### 2.C. Plan evaluation

To evaluate the quality of the treatment plans generated by the three optimization methods, fixed RBE (1.1)-weighted dose-volume histograms (DVHs) and c LETxD-volume histograms were calculated and displayed. The  $D_{98\%}$  and  $D_{2\%}$  of the DVHs in the targets were used to reflect the dose coverage and homogeneity, meanwhile, the  $D_{2\%}$  and  $D_{mean}$  of the DVHs in the OARs were used to assess the risk of exposure. In this study, a given volume, v%, of a structure, receives a dose level, d, or higher could be shown as  $D_{v\%} = d$ . To measure the improvement in the tumor volume coverage and protection of the OARs due to the biological effect, c LETxD<sub>98\%</sub>, c LETxD<sub>2%</sub>, and c LETxD<sub>mean</sub> of the LVHs were compared. All the plans were normalized to have 98% of the CTV covered by the prescribed dose.

### 3. RESULTS

Figure 2 shows the dose-, LETd-, and c LETxD-volume histograms of the CTV and brainstem for the IMPT plans optimized by DoseOpt, LETOpt, and DEAOpt in the brain tumor cases. The doses in the CTV and brainstem generated by the three approaches were comparable. For case 1, the D<sub>2%</sub> in the CTV was 56.67 Gy for the DoseOpt plan, 56.71

Gy for the LETOpt plan, and 56.72 Gy for the DEAOpt plan. The  $D_{2\%}$  in the brainstem was 56.95 Gy for the DoseOpt plan, 56.73 Gy for the LETOpt plan, and 56.75 Gy for the DEAOpt plan. The mean dose in the brainstem was 23.80 Gy, 23.44 Gy, and 23.77 Gy for the DoseOpt, LETOpt, and DEAOpt plans, respectively (Table 2).

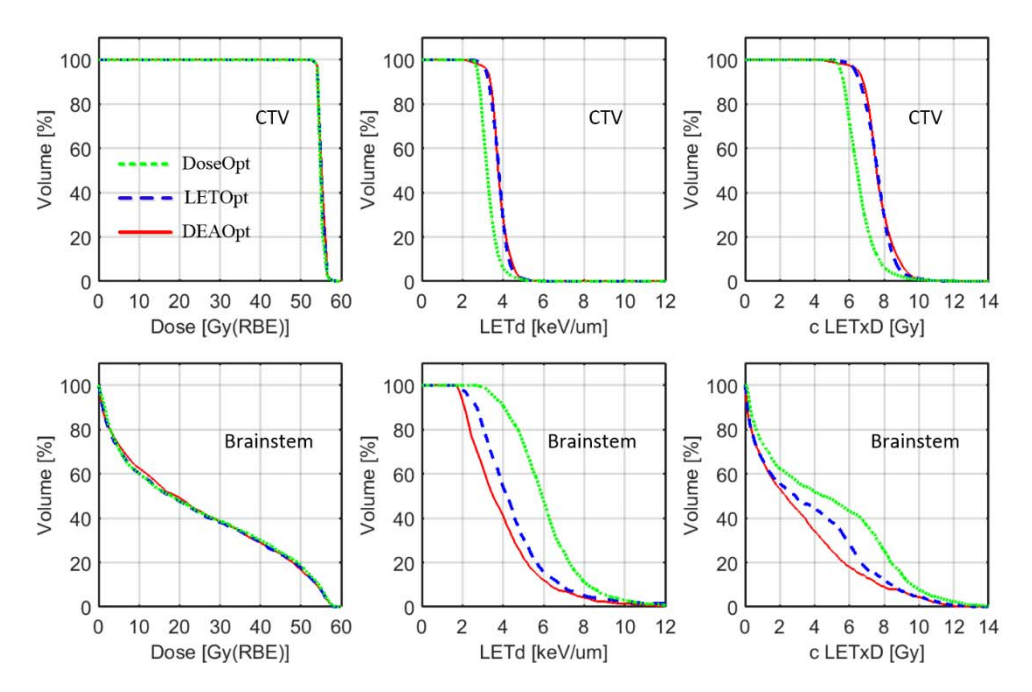


Figure 2. Dose-volume histograms (first column), LET<sub>d</sub>-volume histograms (second

column), and scaled LET-weighted dose (c LETxD)-volume histograms (third column) of the clinical target volume (CTV; top row) and the brainstem (bottom row) for three intensity-modulated proton therapy plans in brain tumor patient case 1. DoseOpt plan (green line), LETOpt plan (blue dashed line), and DEAOpt plan (red line).

Table 2. Dose and linear energy transfer (LET)-weighted dose (LETxD; scaled by  $c = 0.04 \mu m \text{ keV}-1$ ) values in the clinical target volume (CTV) and the brainstem for two brain tumor cases optimized by DoseOpt, LETOpt, and DEAOpt approaches.

Tissue	Dosimetric	Brain tumor case 1			Brain tumor case 2		
	parameters	DoseOpt	LETOpt	DEAOpt	DoseOpt	LETOpt	DEAOpt
CTV	D <sub>98%</sub> (Gy[RBE])	54.00	54.00	54.00	54.00	54.00	54.00
	D <sub>2%</sub> (Gy[RBE])	56.67	56.71	56.72	55.24	55.65	55.76
	c LETxD <sub>98%</sub> (Gy)	5.36	6.08	5.63	4.97	5.94	5.33
	c LETxD <sub>2%</sub> (Gy)	9.06	9.59	9.63	7.30	7.75	8.79
Brainstem	$D_{2\%}$ (Gy[RBE])	56.95	56.73	56.75	56.54	56.73	57.97
	$D_{mean} \left( Gy[RBE] \right)$	23.80	23.44	23.77	36.42	36.83	35.57
	c LETxD <sub>2%</sub> (Gy)	12.31	11.22	10.99	9.66	7.53	8.51
	c LETxD <sub>mean</sub> (Gy)	4.76	3.70	3.19	5.21	3.27	3.45
Calculation Time (s)		176.86	300.48	202.34	394.96	774.40	563.92

Abbreviations: RBE, relative biological effectiveness

In terms of biological effect, both LETOpt and DEAOpt improved the LETd in the CTV and spared it in the brainstem. Since the dose distributions in the target and critical structures were similar for all three methods, the biological effect distributions had the same character as the LETd distributions. The c LETxD<sub>98%</sub> in the CTV was 5.36 Gy for the DoseOpt plan, smaller than the 6.08 Gy for the LETOpt plan and 5.63 Gy for the DEAOpt plan. The c LETxD<sub>2%</sub> in the CTV was 9.06 Gy for the DoseOpt plan, compared to 9.59 Gy and 9.63 Gy for the LETOpt plan and the DEAOpt plan, respectively. For the brainstem, the c LETxD<sub>2%</sub> was 12.31 Gy for the DoseOpt plan, 11.22 Gy for the LETOpt plan, and 10.99 Gy for the DEAOpt plan. The mean value of c LETxD was 4.76 Gy for the DoseOpt plan, higher than the 3.70 Gy for the LETOpt plan and 3.19 Gy for the

Table 3. Dose and linear energy transfer (LET)-weighted dose (LETxD; scaled by c =0.04  $\mu$ m keV-1) values in the clinical target volume (CTV) and the organs at risk (OARs)
for two head and neck (H&N) tumor cases optimized by DoseOpt, LETOpt, and DEAOpt
approaches.

Tissue	Dosimetric	H&N tumor case 1			H&N tumor case 2			
	parameters	DoseOpt	LETOpt	DEAOpt	DoseOpt	LETOpt	DEAOpt	
CTV	D <sub>98%</sub> (Gy[RBE])	66.00	66.00	66.00	66.00	66.00	66.00	
	$D_{2\%}$ (Gy[RBE])	68.39	68.55	68.64	68.36	68.71	69.09	
	c LETxD $_{98\%}$ (Gy)	7.12	7.11	7.17	5.72	6.07	6.28	
	c LETxD $_{2\%}$ (Gy)	11.66	12.11	12.52	8.78	9.40	9.91	
Larynx	$D_{2\%}\left(Gy[RBE]\right)$	53.13	52.90	53.43	66.45	66.69	66.72	
	$D_{mean}$ (Gy[RBE])	5.37	5.12	5.11	10.84	10.92	11.12	
	c LETxD $_{2\%}$ (Gy)	7.13	6.54	6.49	9.90	8.39	8.36	
	c LETxD <sub>mean</sub> (Gy)	0.96	0.81	0.78	1.76	1.38	1.25	
Right	$D_{2\%}\left(Gy[RBE]\right)$	67.21	67.16	67.22	71.09	71.85	72.27	
parotid	D <sub>mean</sub> (Gy[RBE])	6.74	6.67	7.06	17.90	17.99	18.34	
	c LETxD $_{2\%}$ (Gy)	8.38	8.26	8.56	10.94	10.93	10.63	
	c LETxD <sub>mean</sub> (Gy)	0.81	0.81	0.80	2.43	2.39	2.12	
Left	$D_{2\%}(Gy[RBE])$	10.01	9.57	9.29	0.14	0.13	0.07	
parotid	$D_{mean}$ (Gy[RBE])	0.77	0.70	0.67	0.02	0.02	0.02	
	c LETxD $_{2\%}$ (Gy)	0.93	0.76	0.63	0.01	0.01	0.01	
	c LETxD <sub>mean</sub> (Gy)	0.07	0.06	0.05	0.01	0.01	0.00	
Calculation Time (s)		357.34	600.75	402.73	581.58	1044.14	746.23	

284

285

281

The results for brain tumor patient case 2 are shown in Appendix A and Table 2. The differences in dose and c LETxD distributions among the three IMPT plans were similar for the two brain tumor cases.

286

287

288

289

290

291

292

293

294

295

296

297

298

299

300

The improvement in the target coverage and reduction of c LETxD to the critical structures with the LETOpt and DEAOpt plans for the H&N cancer cases was modestly lower than for the brain tumor cases, as illustrated in Figure 3, Table 3, and Appendix B. Compared with DoseOpt plans, the DEAOpt plans reduced the mean value of c LETxD by an average of 23.87% in the larynx for the H&N cancer cases and by an average of 33.38% in the brainstem for the brain tumor cases. Meanwhile, the DEAOpt plans increased the c LETxD<sub>98%</sub> by 5.25% and the c LETxD<sub>2%</sub> by 10.13% on average in the CTV for the H&N cancer cases, lower than the average increment rate of 7.24% for the c LETxD<sub>98%</sub> and 13.35% for the c LETxD<sub>2%</sub> in the brain tumor cases. Thus, the DEAOpt plans improved the biological effect to the same degree as the LETOpt plans in both types of cases. However, the plans were not exactly the same. For example, the LETOpt plan increased the c LETxD<sub>2%</sub> in the CTV to 7.75 Gy, while the DEAOpt plan increased it to 8.79 Gy in brain tumor case 2. In this case, the LETOpt plan achieved a c LETxD<sub>98%</sub> value of 5.94 Gy in the CTV, higher than the 5.33 Gy for the DEAOpt plan.

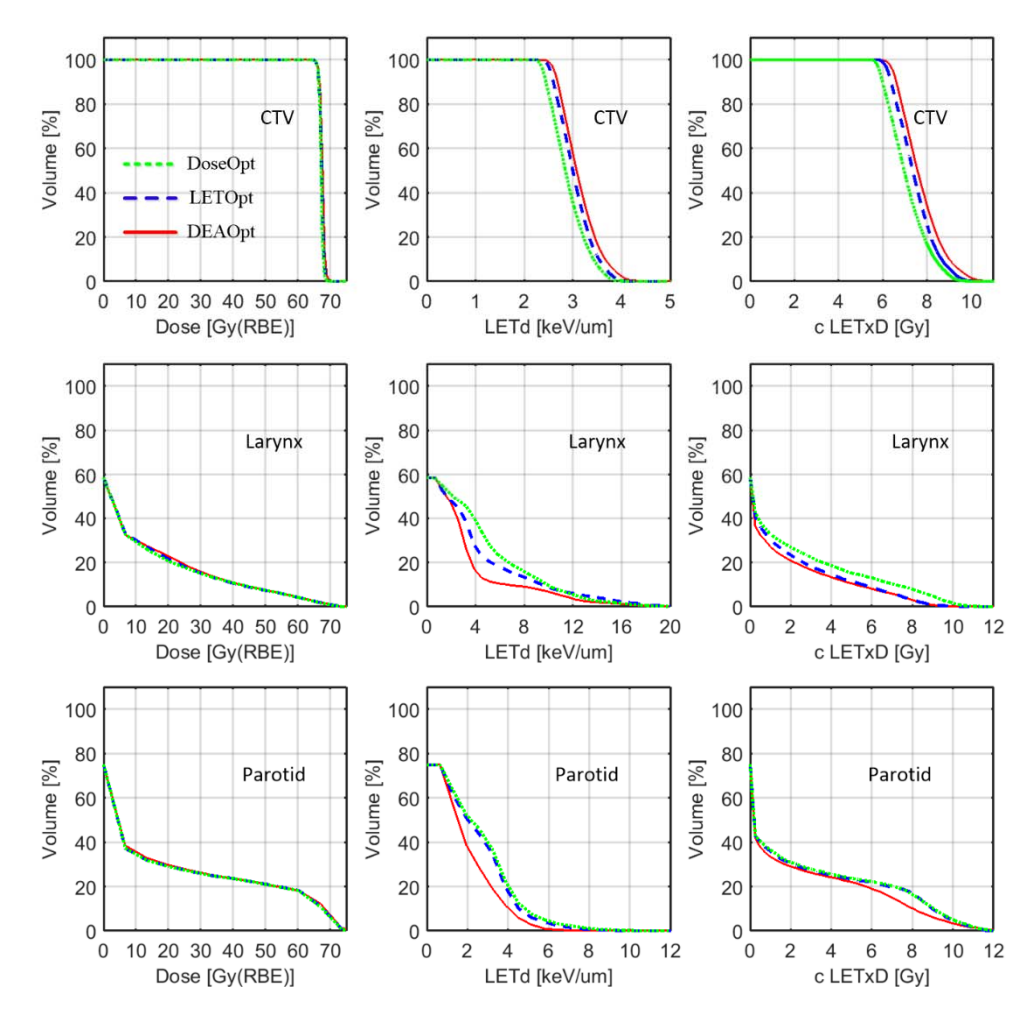


Figure 3. Dose-volume histograms (first column), LETd-volume histograms (second column), and scaled LET-weighted dose (c LETxD)-volume histograms (third column) of the clinical target volume (CTV; top row) and parotid glands (bottom row) for three intensity-modulated proton therapy plans in head and neck cancer patient case 2:.DoseOpt plan (green line), LETOpt plan (blue dashed line), and DEAOpt plan (red line).

Figure 4 shows the dose and biological effect distributions for brain tumor case 1. For physical dose, there was no difference among the three plans. Both the DEAOpt plan and

LETOpt plan avoided the hot spots of c LETxD in the overlap area of the brainstem and

the target. Comparison with the DoseOpt plan also shows that c LETxD in the target improved for both DEAOpt and LETOpt plans. However, it is noteworthy that the DEAOpt plan restricted the high biological effect inside the target border more effectively than did the LETOpt plan, which caused the normal tissue adjacent to the target to receive a lower biological effect.

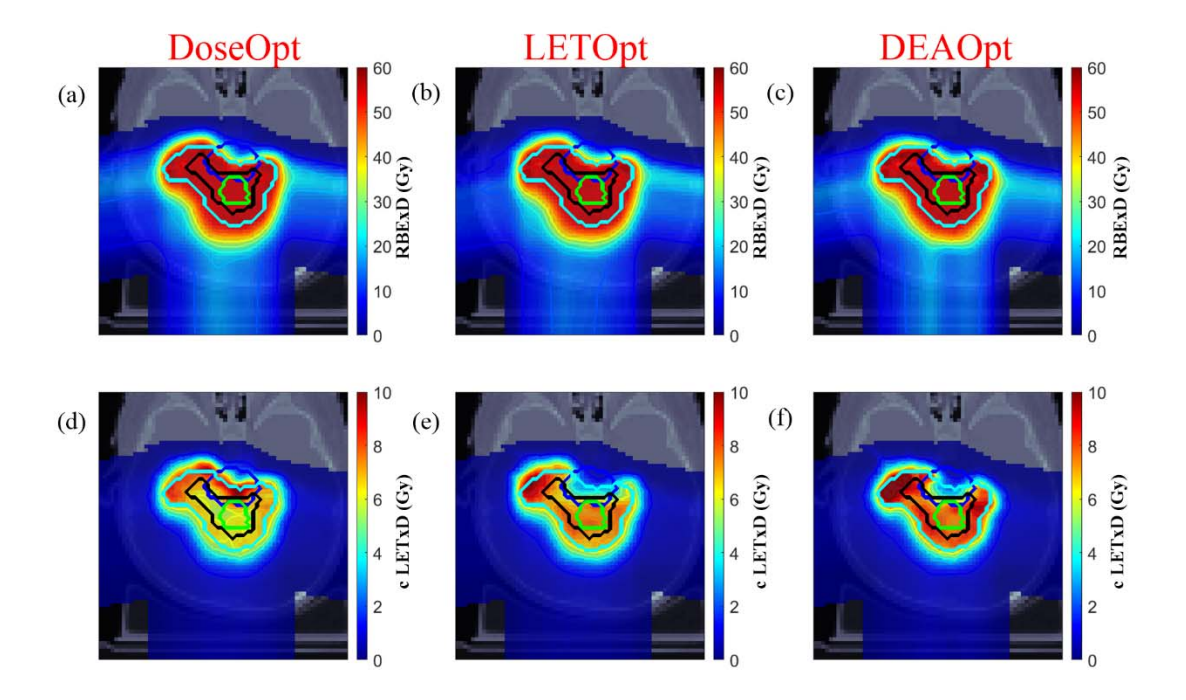


Figure 4. Plan comparison for brain tumor patient case 1. The top row (subfigure a, b and c) shows the dose distributions (based on a constant RBE of 1.1). The bottom row (subfigure d, e and f) shows the distributions of LET-weighted dose scaled by c = 0.04  $\mu$ m keV-1 (c LETxD). The gross target volume, clinical target volume, planning target volume, and brainstem are contoured by green, black, cyan, and blue, respectively.

# 323 4. DISCUSSION

Current LET-based optimization methods <sup>11,13,17,19–21</sup> use LET as a surrogate for RBE optimization <sup>11,21</sup> because of the considerable uncertainties in the validity of RBE models and the almost linear relationship between LET and RBE. <sup>18</sup> In addition, the high degree of freedom of the IMPT plan makes it feasible to produce satisfactory dose distributions while achieving desirable LET distributions. <sup>20</sup> However, a drawback to the existing methods is that they use the inverse planning approach to optimize the LET distribution, which adds extra complexity, <sup>27</sup> requiring calculation and evaluation of LET<sub>d</sub> or LETxD in each iteration of the optimization process. To overcome this challenge, our method includes a regularization term for each scanning spot to reduce the complexity of the first and second derivatives.

The runtime of DEAOpt was, on average, 30.37% faster than that of LETOpt and 24.52% slower than that of DoseOpt (Table 2 and Table 3). The boost of computing time did not sacrifice plan quality; the DEAOpt plan's biological effect and physical dose distributions were comparable with those of the LETOpt plan. Regarding treatment plan quality, i.e., physical dose and biological effect distributions, DEAOpt performed similarly as, or slightly better than, LETOpt. Although the present feasibility study cannot render a statistical power on superiority of either method, DEAOpt is shown to be a straightforward alternative to other inverse LET optimization approaches in order to avoid high LET in critical structures and normal tissues.

In proton beams, LET continues to increase beyond the Bragg peak. We classified the scanning spots into four categories according to the topological relationship between their peak LETxD positions and different organs of interest (Figure 1). In Situation A, the peak LETxD position falls into the OAR area and outside the target region, meaning that the dose intensity in this scanning spot may aggravate toxicities in critical structures. Of course, this scanning spot also contributes to the dose in the border of the target, but it can be replaced by other scanning spots from different beams. In Situation B, where the peak LETxD position is in the overlap area of the target and OARs, the priority of treatment planning decides the penalty set. For example, if the first priority is to kill the tumor cells, we allow for a high biological effect in this area, which makes the penalty in this scanning spot close to 0; if protecting critical structures is the priority, a high penalty should be assigned to this scanning spot to restrain the biological effect in this area. For other situations, the peak LETxD position's radius may cover the edge of OARs or the target. When the irradiated region overlaps with the target, the corresponding scanning spot will guarantee the homogeneity and coverage of physical dose in the tumor. Sometimes, when the overlap is with OARs, we should limit the intensity in this scanning spot. If the peak LETxD position is far away from all OARs and target, a high penalty should be set for this scanning spot to protect healthy tissues.

345

346

347

348

349

350

351

352

353

354

355

356

357

358

359

360

361

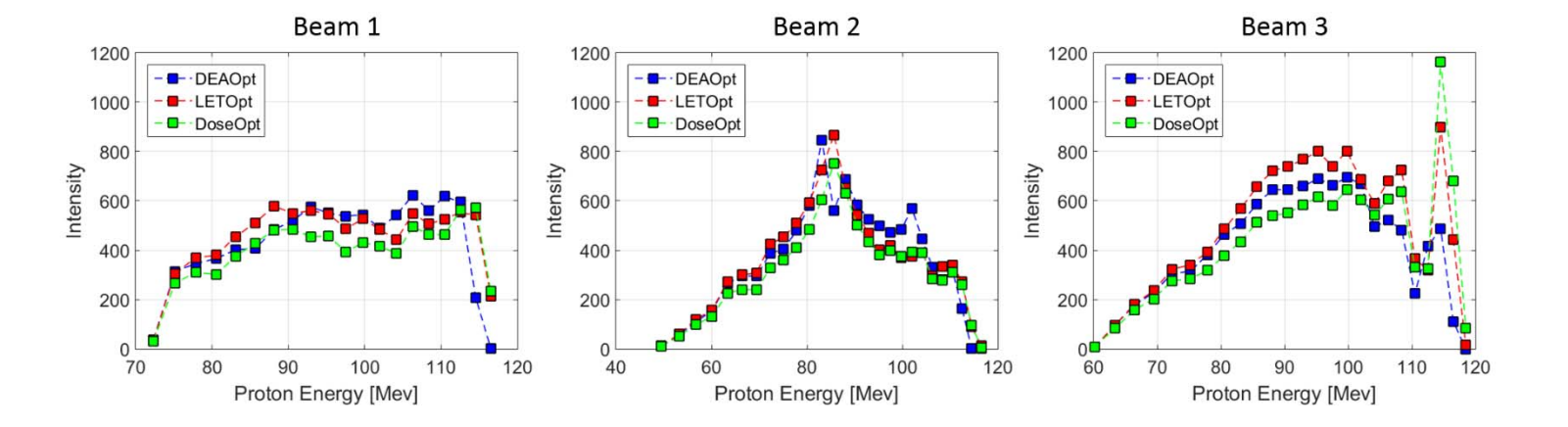


Figure 5. Comparisons of the intensity in each proton energy layer for three beams with the DEAOpt plan, LETOpt plan, and DoseOpt plan in head and neck tumor case 2.

Regardless of the optimization approach used to optimize the physical dose and LET, the objective is achieved mostly by shifting LET hot spots to other regions nearby or inside the target. Conventional treatment planning usually places the Bragg peaks at the distal edge of the target to maintain the dose coverage, which inevitably causes the region of high LET to be located in the periphery of the target. To keep protons stopping within the target region, location of the scanning spot at the distal edge of the target should be avoided. This would protect the normal tissue adjacent to the target from the risk of side effects associated with high LET. As shown in Figure 5, the DEAOpt plan deposits lower intensity at the last two proton energies in each beam than do the LETOpt and DoseOpt plans. Points in these two energy layers have the potential to release LET outside of the target. Nonetheless, there was no substantial difference in total intensity among the three

plans, for which their dose distributions were similar. In this example, the total spot intensity from all spots of all beams was 28477.4, 30498.6 and 29232.3 for the DoseOpt LETOpt and DEAOpt plan, respectively. In other words, the DoseOpt plan indicates slightly fewer monitor units delivered than the other plans.

Our research confirmed that biological effect optimization can be achieved by optimizing the location of scanning spots directly instead of using the inverse optimization method. The effectiveness of DEAOpt is highly dependent on the geometry of structures and the spot arrangement. As shown by Figure 5, our method tends to avoid spots in the beam distal edge because of the trade-off effect between dose and LET. In our H&N cancer cases, the DEAOpt method made a smaller difference than in our brain tumor cases because more OARs need to be protected during irradiation of H&N tumors. This phenomenon was also observed with the LETOpt plans.

Although variable RBE has not been adopted in the clinical setting of proton therapy, the DEAOpt method could be readily adapted to an efficient alternative to variable RBE optimization given a designated RBE model. To do so, peak positions of variable RBE weighted dose (RBExD), instead of LETxD, are evaluated and optimized. For example, Figure 6 shows predicted RBExD based on three phenomenological RBE models (Carabe et al<sup>6</sup>, Wedenberg et al<sup>7</sup>, McNamara et al<sup>8</sup>) and cLETxD at three proton energies. Because DEAOpt only needs to calculate RBE once prior to optimization iterations, its

computational efficiency would be comparable to conventional optimization approaches

## (RBE=1.1) as demonstrated in this study.

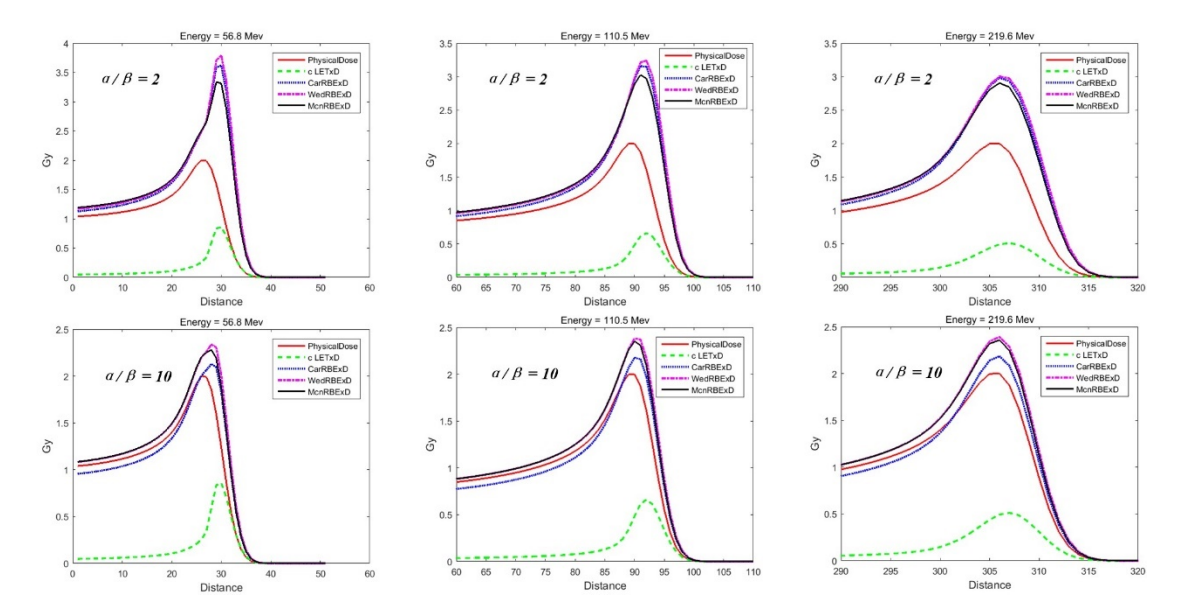


Figure 6. Predicted variable RBE weighted dose (RBExD) based on three

phenomenological RBE models (Carabe, Wedenberg and McNamara) and cLETxD (c =  $0.04~\mu m~keV-1$ ) at three selected proton energies (56.8, 110.5 and 219.6 MeV) based on  $\alpha/\beta=2$  and  $\alpha/\beta=10$ .

One of the limitations of the DEAOpt method is that it does not explicitly optimize the biological effect, or LETxD, distribution in the target. In order to do so, this method may be extended by adding negative penalties to the spots that are not identified to have normal tissue LET penalties, i.e., increasing LET in target. More importantly, DEAOpt could be used to provide a good starting point for IMPT biological optimization when prescriptions in terms of LET or RBE are possible in future clinical use.

Another limitation of DEAOpt in this study is the manual setting of penalty weights for spot locations. Future improvement is needed to automate these weights to mitigate human dependence and increase effenciency. Currently, from our experience, the trial-and-error iterations of setting optimization parameters for this method were, at least, not more than the LET-based method that we implemented. For parameters specific in the DEAOpt method  $(\theta)$ , we found that a good starting point for the set of parameters  $(\theta_A, \theta_C, \theta_B, \theta_D)$  could be (5, 1, 0.2, 0.1) for the cases included in our study. Nevertheless, biological optimization methods are generally more complex than standard ones that only optimizes physical dose, in terms of setting more input parameters, because of the tradeoff effect between physical dose and biological effect. To overcome this issue, auto-planning approaches and multi-criteria optimization become even more important. It is worth noting that the present study is based on matRad's analytical dose and LET calculations, as well as a specific optimizer. It is possible the findings may differ if we used a different system. In Appendix C, we observed differences in dose and LET between two plans optimized in matRad and in an in-house Monte Carlo system<sup>20</sup>. In addition, the accuracy of LET calculation in matRad is limited due to the assumption of constant LET in lateral direction and excluding secondary protons.<sup>†</sup> This could lead to inaccuracy in determining the peak positions of cLETxD calculated in DEAOpt.

Nevertheless, the purpose of the present study was to explore an computationally efficient

planning approach with considerations of proton biological effect, and the DEAOpt

414

415

416

417

418

419

420

421

422

423

424

425

426

427

428

429

430

431

432

433

methodology is independent from dose/LET engines. We will test its generality in our in-house Monte Carlo simulation and optimization system<sup>20,22</sup> in the next study.

Furthermore, the plans optimized here were not necessarily robust to treatment delivery uncertainties, even though DEAOpt plans tend to avoid locating high-intensity spots near the interface region between target and OARs, which should be in favor of plan robustness especially against beam range uncertainty. Thus, incorporating DEAOpt into an IMPT robust optimization framework could be straightforward and will be investigated in our future work.

### 5. CONCLUSION

In this study, we proposed and developed a distal-edge avoidance-guided optimization method to optimize IMPT plans in terms of their LETxD distributions without degrading the physical dose distributions, which are comparable to those of LET optimization plans. We used an influence index to quantify the contribution of the biological effect from each scanning spot on the basis of its topological relationship to different organs of interest. This method could be especially beneficial for patient cases where critical structures are adjacent to the target area. In addition, the DEAOpt approach is less complex computationally and therefore faster than the LETOpt approach.

### REFERENCES

- 1. Lomax AJ, Boehringer T, Coray A, et al. Intensity modulated proton therapy: A
- 457 clinical example. *Med Phys.* 2001;28(3):317-324. doi:10.1118/1.1350587
- 2. Paganetti H, Niemierko A, Ancukiewicz M, et al. Relative biological effectiveness
- 459 (RBE) values for proton beam therapy. *Int J Radiat Oncol Biol Phys*.
- 460 2002;53(2):407-421. doi:10.1016/S0360-3016(02)02754-2
- 461 3. Kohno R, Cao W, Yepes P, et al. Biological dose comparison between a fixed
- RBE and a variable RBE in SFO and MFO IMPT with various multi-beams for
- brain cancer. Int J Med Physics, Clin Eng Radiat Oncol. 2019;08(01):32-45.
- doi:10.4236/ijmpcero.2019.81004
- 465 4. International Commission on Radiation Units and Measurements. Prescribing,
- recording, and reporting photon-beam IMRT. *J ICRU*. 2010;10(1):7-16.
- doi:10.1093/jicru/ndq006
- 468 5. Giovannini G, Böhlen T, Cabal G, et al. Variable RBE in proton therapy:
- comparison of different model predictions and their influence on clinical-like
- 470 scenarios. *Radiat Oncol.* 2016;11(1):68. doi:10.1186/s13014-016-0642-6
- 6. Carabe-Fernandez A, Dale RG, Jones B. The incorporation of the concept of
- minimum RBE (RBEmin) into the linear-quadratic model and the potential for
- improved radiobiological analysis of high-LET treatments. *Int J Radiat Biol.*
- 474 2007;83(1):27-39. doi:10.1080/09553000601087176
- 475 7. Wedenberg M, Lind BK, Hårdemark B. A model for the relative biological

- effectiveness of protons: The tissue specific parameter  $\alpha / \beta$  of photons is a
- predictor for the sensitivity to LET changes. *Acta Oncol (Madr)*.
- 478 2013;52(3):580-588. doi:10.3109/0284186X.2012.705892
- 479 8. McNamara AL, Schuemann J, Paganetti H. A phenomenological relative
- biological effectiveness (RBE) model for proton therapy based on all published *in*
- *vitro* cell survival data. *Phys Med Biol*. 2015;60(21):8399-8416.
- doi:10.1088/0031-9155/60/21/8399
- 483 9. Carabe-Fernandez A, Moteabbed M, Depauw N, Paganetti H. Range uncertainty in
- proton therapy due to variable biological effectiveness. *Med Phys.*
- 485 2011;38(6):3639. doi:10.1118/1.3612611
- 486 10. Giantsoudi D, Unkelbach J, Botas P, Grassberger C, Paganetti H. Can robust
- optimization for range uncertainty in proton therapy act as a surrogate for
- biological optimization? *Int J Radiat Oncol Biol Phys.* 2017;99(2):S106-S107.
- doi:10.1016/j.ijrobp.2017.06.253
- 490 11. Unkelbach J, Botas P, Giantsoudi D, Gorissen BL, Paganetti H. Reoptimization of
- intensity modulated proton therapy plans based on linear energy transfer. Int J
- 492 Radiat Oncol Biol Phys. 2016;96(5):1097-1106. doi:10.1016/j.ijrobp.2016.08.038
- 493 12. Paganetti H. Relative biological effectiveness (RBE) values for proton beam
- 494 therapy. Variations as a function of biological endpoint, dose, and linear energy
- 495 transfer. *Phys Med Biol*. 2014;59(22):R419-R472.
- doi:10.1088/0031-9155/59/22/R419

- 497 13. Fager M, Toma-Dasu I, Kirk M, et al. Linear energy transfer painting with proton
- therapy: A means of reducing radiation doses with equivalent clinical effectiveness.
- 499 *Int J Radiat Oncol Biol Phys.* 2015;91(5):1057-1064.
- doi:10.1016/j.ijrobp.2014.12.049
- 501 14. Wilkens JJ, Oelfke U. Analytical linear energy transfer calculations for proton
- therapy. *Med Phys.* 2003;30(5):806-815. doi:10.1118/1.1567852
- 503 15. Bassler N, Jäkel O, Søndergaard CS, Petersen JB. Dose-and LET-painting with
- particle therapy. *Acta Oncol (Madr)*. 2010;49(7):1170-1176.
- 505 doi:10.3109/0284186X.2010.510640
- 506 16. Wan Chan Tseung HS, Ma J, Kreofsky CR, Ma DJ, Beltran C. Clinically
- applicable Monte Carlo-based biological dose optimization for the treatment of
- head and neck cancers with spot-scanning proton therapy. *Int J Radiat Oncol Biol*
- 509 *Phys.* 2016;95(5):1535-1543. doi:10.1016/j.ijrobp.2016.03.041
- 510 17. Traneus E, Ödén J. Introducing proton track-end objectives in intensity modulated
- proton therapy optimization to reduce linear energy transfer and telative biological
- effectiveness in critical structures. *Int J Radiat Oncol Biol Phys.*
- 513 2019;103(3):747-757. doi:10.1016/j.ijrobp.2018.10.031
- 514 18. Giantsoudi D, Grassberger C, Craft D, Niemierko A, Trofimov A, Paganetti H.
- Linear energy transfer-guided optimization in intensity modulated proton therapy:
- Feasibility study and clinical potential. *Int J Radiat Oncol Biol Phys.*
- 517 2013;87(1):216-222. doi:10.1016/j.ijrobp.2013.05.013

- 518 19. Inaniwa T, Kanematsu N, Noda K, Kamada T. Treatment planning of intensity
- modulated composite particle therapy with dose and linear energy transfer
- optimization Treatment planning of intensity modulated composite particle therapy
- with dose and linear energy transfer optimization. *Phys Med Biol*.
- 522 2017;62(12):5180-5197.
- 523 20. Cao W, Khabazian A, Yepes PP, et al. Linear energy transfer incorporated
- intensity modulated proton therapy optimization. *Phys Med Biol.*
- 525 2018;63(1):15013. doi:10.1088/1361-6560/aa9a2e
- 526 21. An Y, Shan J, Patel SH, et al. Robust intensity-modulated proton therapy to reduce
- high linear energy transfer in organs at risk. *Med Phys.* 2017:1-10.
- 528 doi:10.1002/mp.12610
- 529 22. Bai X, Lim G, Wieser H, et al. Robust optimization to reduce the impact of
- biological effect variation from physical uncertainties in intensity-modulated
- proton therapy. *Phys Med Biol*. 2019;64(2):025004. doi:10.1088/1361-6560/aaf5e9
- 532 23. Lomax AJ. Intensity modulation methods for proton radiotherapy. *Phys Med Biol*.
- 533 1999;44(1):185–205. doi:10.1088/0031-9155/44/1/014
- 534 24. Wieser H, Cisternas E, Wahl N, et al. Development of the open-source dose
- calculation and optimization toolkit matRad. *Phys Med Biol*.
- 536 2017;44(6):2556-2568. doi:10.1002/mp.12251
- 537 25. Hong L, Goitein M, Bucciolini M, et al. A pencil beam algorithm for proton dose
- calculations. *Phys Med Biol.* 1996;41(8):1305-1330.

- doi:10.1088/0031-9155/41/8/005
- 540 26. Bortfeld T. Optimized planning using physical objectives and constraints. Semin
- 541 *Radiat Oncol.* 1999;9(1):20-34. doi:10.1016/S1053-4296(99)80052-6
- 542 27. Oelfke U, Bortfeld T. Inverse planning for photon and proton beams. *Med Dosim*.
- 543 2001;26(2):113-124. doi:10.1016/S0958-3947(01)00057-7
- Wang Q, Johnson A, Yepes P, et al. Validation of the fast dose calculator for
- Shanghai Proton and Heavy Ion Center. *Biomed Phys Eng Express*.
- 546 2018;4(6):065007. doi:10.1088/2057-1976/aae039
- 547 29. Chen W, Unkelbach J, Trofimov A, et al. Including robustness in multi-criteria
- optimization for intensity-modulated proton therapy. *Phys Med Biol*.
- 549 2012;57(3):591-608. doi:10.1088/0031-9155/57/3/591
- 550 30. Wächter A, Biegler LT. On the Implementation of an Interior-Point Filter
- Line-Search Algorithm for Large-Scale Nonlinear Programming. Vol 106.; 2006.
- doi:10.1007/s10107-004-0559-y

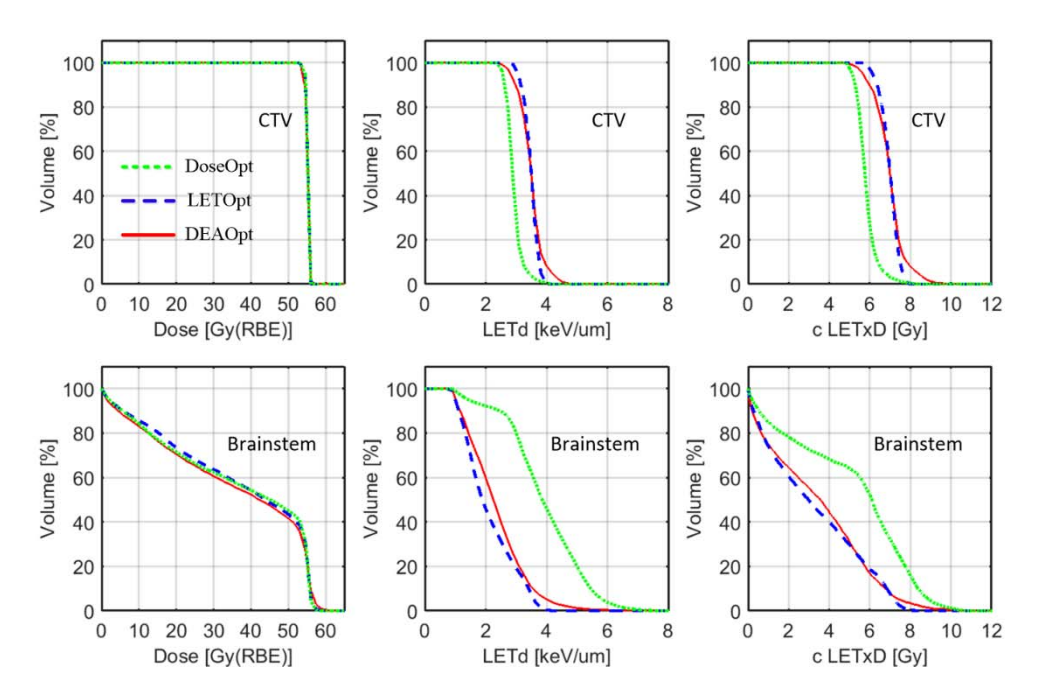
# 554 **ACKNOWLEDGMENTS**

- This work was partly supported by the National Cancer Institute of the National Institutes
- of Health (2U19CA021239-35) and the Cancer Prevention and Research Institute of Texas
- 557 (RP160232). Editorial support was provided by Amy Ninetto of Scientific Publications
- 558 Services, Research Medical Library, The University of Texas MD Anderson Cancer
- 559 Center.

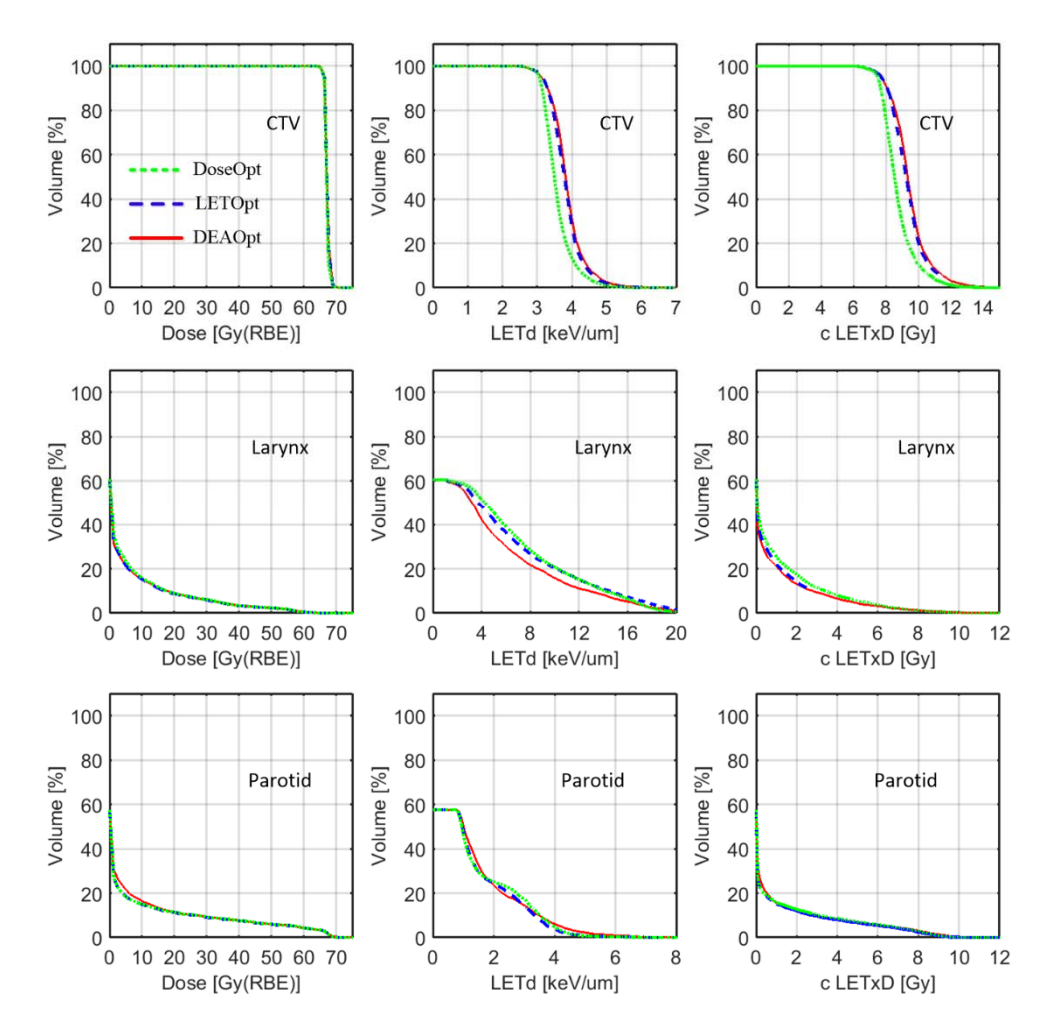
# CONFLICT OF INTEREST DISCLOSURES

The authors have no relevant conflict of interests to disclose.

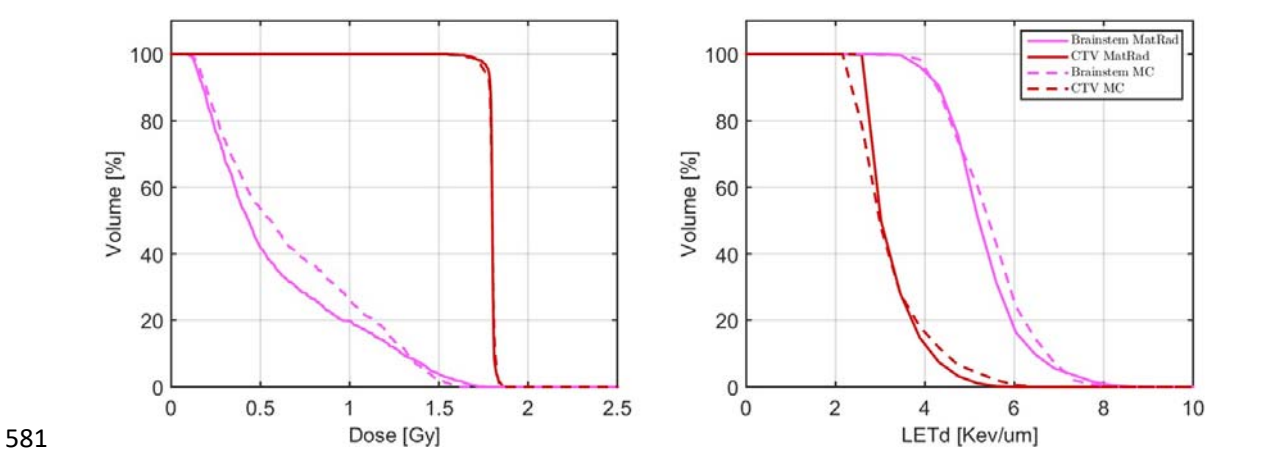
### 564 Appendices



Appendix A. Dose-volume histograms (first column), LET<sub>d</sub>-volume histograms (second column), and scaled LET-weighted dose (c LETxD)-volume histograms (third column) of the clinical target volume (CTV; top row) and the brainstem (bottom row) for three intensity-modulated proton therapy plans in brain tumor patient case 2. DoseOpt plan (green line), LETOpt plan (blue dashed line), and DEAOpt plan (red line).



Appendix B. Dose-volume histograms (first column), LETd-volume histograms (second column), and scaled LET-weighted dose (c LETxD)-volume histograms (third column) of the clinical target volume (CTV; top row) and the organs at risk (larynx, middle row; parotid gland, bottom row) for three intensity-modulated proton therapy plans in head and neck tumor patient case 1. DoseOpt plan (green line), LETOpt plan (blue dashed line), and DEAOpt plan (red line).



Appendix C. Dose-volume histograms (left),  $LET_d$ -volume histograms (right) of the clinical target volume (CTV) and the brainstem of matRad (solid lines) and Monte Carlo (dashed lines) optimized plans for brain tumor patient case 1.